Intelligence 37 (2009) 124–135

Contents lists available at ScienceDirect

Intelligence

Gray matter correlates of fluid, crystallized, and spatial intelligence: Testing the P-FIT model

Roberto Colom [a,*], Richard J. Haier [b], Kevin Head [b], Juan Álvarez-Linera [c], María Ángeles Quiroga [d], Pei Chun Shih [a], Rex E. Jung [e]

[a] Universidad Autónoma de Madrid (UAM), Spain
[b] University of California, Irvine (UCI), USA
[c] Hospital Ruber Internacional, Madrid, Spain
[d] Universidad Complutense de Madrid (UCM), Spain
[e] The Mind Institute, Albuquerque, USA

ARTICLE INFO

Article history:
Received 16 April 2008
Received in revised form 25 July 2008
Accepted 29 July 2008
Available online 18 September 2008

Keywords:
Neuroanatomy
General intelligence
Fluid intelligence
Crystallized intelligence
Spatial intelligence
Voxel-based Morphometry
Frontal lobes
Parietal lobes
MRI

ABSTRACT

The parieto-frontal integration theory (P-FIT) nominates several areas distributed throughout the brain as relevant for intelligence. This theory was derived from previously published studies using a variety of both imaging methods and tests of cognitive ability. Here we test this theory in a new sample of young healthy adults (N = 100) using a psychometric battery tapping fluid, crystallized, and spatial intelligence factors. High resolution structural MRI scans (3T) were obtained and analyzed with Voxel-based Morphometry (VBM). The main findings are consistent with the P-FIT, supporting the view that general intelligence (g) involves multiple cortical areas throughout the brain. Key regions include the dorsolateral prefrontal cortex, Broca's and Wernicke's areas, the somato-sensory association cortex, and the visual association cortex. Further, estimates of crystallized and spatial intelligence with g statistically removed, still share several brain areas with general intelligence, but also show some degree of uniqueness.

Individual differences in intelligence result from both genetic and non-genetic factors. Making a key point for the genetic view, Kovas and Plomin (2006) have proposed the "generalist genes hypothesis". This hypothesis states that the expression of genes is distributed throughout the brain, not localized in any discrete region. For the non-genetic view, Garlick (2003) has argued that intelligence differences derive from the development of neural connections in response to environmental challenges.

Genetic and non-genetic factors and their interactions impact brain structure (Draganski et al., 2004; Posthuma et al., 2003; Thompson et al., 2001). Haier and colleagues have shown that variation in structures throughout the brain was related to intelligence (Colom, Jung, & Haier, 2006a,b, 2007; Johnson, Jung, Colom, & Haier, 2008; Haier, Jung, Yeo, Head, & Alkire, 2004, 2005) finding that (1) there are significant associations between brain variations in gray matter (GM) density across discrete areas of the frontal, parietal, temporal, and occipital lobes, and IQ scores, (2) there are pronounced age and sex differences, and (3) the associations are distinguishable for IQ, the g factor, and cognitive abilities orthogonal to IQ (Colom, 2007; Johnson et al., 2008). Toga and Thompson (2005, 2007) also have discussed how structural brain mapping could increase our understanding of intelligence.

Recently, Jung and Haier (2007) have proposed the parieto-frontal integration theory (P-FIT) of intelligence after the consideration of 37 neuroimaging studies published between 1988 and 2007. The P-FIT model is consistent with the generalist genes hypothesis mentioned above (Kovas &

* Corresponding author. Facultad de Psicología, Universidad Autónoma de Madrid, 28049 Madrid, Spain. Tel.: +34 91 497 41 14.
E-mail address: roberto.colom@uam.es (R. Colom).

0160-2896/$ – see front matter © 2008 Elsevier Inc. All rights reserved.
doi:10.1016/j.intell.2008.07.007

Plomin, 2006), because several regions distributed across the entire cerebral cortex and within discrete white matter regions are identified. These P-FIT regions generally imply distinguishable information processing stages (Fig. 1):

1. In the first stage, temporal and occipital specific areas process sensory information: the extrastriate cortex (Brodmann areas –BAs– 18 and 19) and the fusiform gyrus (BA 37), involved with recognition, imagery and elaboration of visual inputs, as well as the Wernicke's area (BA 22) for analysis and elaboration of syntax of auditory information.
2. The second stage implicates integration and abstraction of this information by parietal BAs 39 (angular gyrus), 40 (supramarginal gyrus), and 7 (superior parietal lobule).
3. In the third stage, these parietal areas interact with the frontal lobes, which serve to problem solve, evaluate, and hypothesis test. Frontal BAs 6, 9, 10, 45, 46, and 47 are underscored by the theoretical model.
4. Finally, the anterior cingulate (BA 32) is implicated for response selection and inhibition of alternative responses, once the best solution is determined in the previous stage.

White matter (WM), especially the arcuate fasciculus, plays a critical role for a reliable communication of information across these brain processing units.

Jung and Haier (2007) posit that not all these brain areas are equally necessary in all individuals for intelligence. They predict that discrete brain regions of the dorsolateral prefrontal cortex (BAs 9, 45, 46, and 47) and the parietal cortex (BAs 7 and 40) may be key for the core of general intelligence.

Whereas the P-FIT stressed the commonalities among studies, Colom (2007) noted the great variability among the studies summarized by Jung and Haier (2007). Only a very small number of discrete brain areas approach 50% of convergence across published studies employing the same neuroimaging strategy: (a) structural studies nominate 32 brain areas, but only BAs 39–40 and 10 approach 50% of convergence; (b) PET studies nominate 22 brain areas, but only BAs 18–19 and 46–47 enjoy 50% of convergence; (c) *f*MRI studies nominate 26 brain areas, but only BAs 6, 9, 7, 40, and 19 reach 50% of convergence.

Why is the evidence so heterogeneous? Most neuroimaging studies of intelligence are limited by small sample sizes, wide age ranges, and a broad variety of individual tests used to assess cognitive abilities (Haier & Jung, 2007). The purpose of the present paper is to test the main aspects of the P-FIT in a new sample of one hundred young healthy participants of both sexes and a small age range using a psychometric battery tapping fluid, crystallized, and spatial intelligence.

1. Method

1.1. Participants

405 university undergraduates were recruited from the *Universidad Autónoma de Madrid* and the *Universidad Complutense de Madrid*. They completed a battery of nine tests measuring intelligence. A sample of 120 Ss was randomly selected for MRI scanning (60 males and 60 females). 104 volunteered to participate in the study, but 4 scans were of insufficient quality for analyses. Therefore, the final sample was comprised of 100 Ss (56 females and 44 males, mean age = 19.9, SD = 1.7, age range = 18 to 27). Ninety three Ss were right-handed.

All Ss gave informed written consent. Participants completed a questionnaire asking for medical, neurological, and psychiatric illness, or conditions that would be contra-indicated for undertaking MRI scans. They received a payment of 20 € for participation.

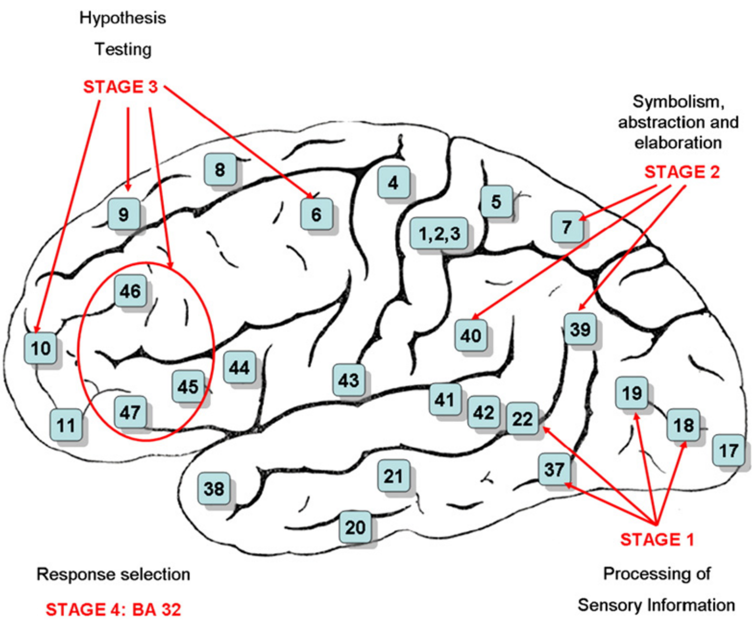

Fig. 1. Processing stages associated with specific brain regions according to the P-FIT model: processing of sensory information (stage 1), symbolism, abstraction, and elaboration (stage 2), hypothesis testing (stage 3), and response selection (stage 4). The arcuate fasciculus (i.e. the neural pathway connecting the posterior part of the temporo-parietal junction with the frontal cortex) is not shown in the figure, but also underscored by the P-FIT model.

1.2. Intelligence measures

Intelligence was measured by nine tests tapping fluid, crystallized, and spatial cognitive abilities. These tests belonged to the same psychometric battery employed in the Colom et al.'s (in press) study 3.

Fluid intelligence (Gf) was measured by the Advanced Progressive Matrices Test (APM, screening version, even numbered items), the inductive reasoning subtest (R) from the Primary Mental Abilities (PMA) Battery, and the abstract reasoning (AR) subtest from the Differential Aptitude Test (DAT-5) Battery (screening version, even numbered items).

The *APM* comprises a matrix figure with three rows and three columns with the lower right hand entry missing. Participants must choose, among eight alternatives, the one completing the 3×3 matrix figure. The score is the total number of correct responses.

DAT-AR is a series test based on abstract figures. Each item includes four figures following a given rule, and the participant must choose one of five possible alternatives. The score is the total number of correct responses.

PMA-R comprises letters' series items. The rule (or rules) underlying a given sequence of letters [*a-c-a-c-a-c-a-c*] must be extracted in order to select a given letter from a set of six possible alternatives [*a-b-c-d-e-f*]. Only one alternative is correct. The score is the total number of correct responses.

Crystallized intelligence (Gc) was measured by the verbal reasoning (VR) and the numerical reasoning (NR) subtests from the DAT-5 (screening versions, even numbered items), as well as by the vocabulary (V) subtest from the PMA.

DAT-VR is a verbal reasoning test. A given sentence stated like an analogy must be completed. The first and last words from the sentence are missing, so a pair of words must be selected to complete the sentence from five possible alternative pairs of words. For instance: *… is to water like eating is to… (A) Travelling-Driving, (B) Foot-Enemy, (C) Drinking-Bread, (D) Girl-Industry, (E) Drinking-Enemy*. Only one alternative is correct. The score is the total number of correct responses.

DAT-NR consists of quantitative reasoning problems. For instance:

Which number must be substituted by the letter P if the sum is correct?

$5P+2=58$

(A) 3, (B) 4, (C) 7, (D) 9, (E) None of them

The score is the total number of correct responses.

PMA-V is a synonym test. The meaning of four alternative words must be evaluated against a given word that serves as model. For instance, *STOUT: Sick–Fat–Short–Rude*. Only one alternative is correct. The score is the total number of correct responses.

Spatial intelligence (Gv) was measured by the rotation of solid figures test, the mental rotation (S) subtest from the PMA, and the spatial relations (SR) subtest from the DAT-5 (screening version, even numbered items).

Rotation of solid figures. Each item includes a model figure and five alternatives must be evaluated against it. The participant must evaluate which alternative can be rotated within a 3D space to fit the model figure. Only one alternative is correct. The score is the total number of correct responses.

PMA-S. Each item includes a model figure and six alternatives must be evaluated against it. Some alternatives are simply rotated versions of the model figure, whereas the remaining figures are mirror imaged. Only the rotated figures must be selected. Several alternatives could be correct for each item. The score is the total number of correct responses (appropriately selected figures —simply rotated) minus the total number of incorrect responses (inappropriately selected figures —mirror imaged).

DAT-SR is a mental folding test. Each item is composed by an unfolded figure and four folded alternatives. The unfolded figure is shown at the left, whereas figures at the right depict folded versions. Participants are asked to choose one folded figure matching the unfolded figure at the left. The score is the total number of correct responses (well chosen folded figures).

1.3. MRI data collection

MRIs were obtained with a 3T scanner (GEHC Waukesha, WI, 3T Excite HDX) 8-channels coil. 3D: FSPGR with IR preparation pulse (TR 5.7 ms, TE 2.4 ms TI 750 ms, flip angle 12). Sag acquisition .8 mm thickness, full brain coverage (220 slices), matrix 266×266 FOV 24 (isotropic voxels .7 cm^3).

1.4. MRI data analyses

We applied Voxel-based Morphometry (VBM) to identify brain areas where GM volumes were correlated to intelligence. We used Statistical Parametric Mapping software (SPM5; The Wellcome Department of Imaging Neuroscience, University College London) to apply the optimized VBM protocol to the sample using the methods of Ashburner and Friston (2000) and Good et al. (2001). To preserve the amount of tissue in any given anatomical region after spatial normalization, the optimal GM partitions were multiplied by the Jacobian determinants of their respective spatial transformation matrix. This modulation step is to allow the final VBM statistics to reflect local deviations in the absolute amount (volume) of tissue in different regions of the brain (Ashburner & Friston, 2000). The modulated GM partitions were then smoothed with a 12-mm FWHM isotropic Gaussian kernel to account for slight misalignments of homologous anatomical structures and to ensure statistical validity under parametric assumptions. Each individual scan was finally fitted to a standardized SPM template specifically created for 3T MRI scans (tissue probability map provided by the International

Table 1
Descriptive statistics and correlation matrix

	1	2	3	4	5	6	7	8	9
1. APM		.40**	.47**	.15	.20*	.28**	.24*	.08	.22*
2. PMA-R			.37**	.24*	.29**	.32**	.13	.11	.27**
3. DAT-AR				.21*	.31**	.34**	.35**	.19*	.37**
4. PMA-V					.30**	.31**	.20*	.22*	−.01
5. DAT-VR						.34**	.11	.08	.24*
6. DAT-NR							.20*	.11	.19
7. Solid. fig.								.41**	.41**
8. PMA-S									.32**
9. DAT-SR									
Mean	11.8	19.5	14.4	32.7	13.6	11.9	9.0	27.5	15.9
SD	2.4	4.5	3.5	6.6	3.0	3.2	3.9	9.7	4.8

*$p<.05$.
**$p<.01$.

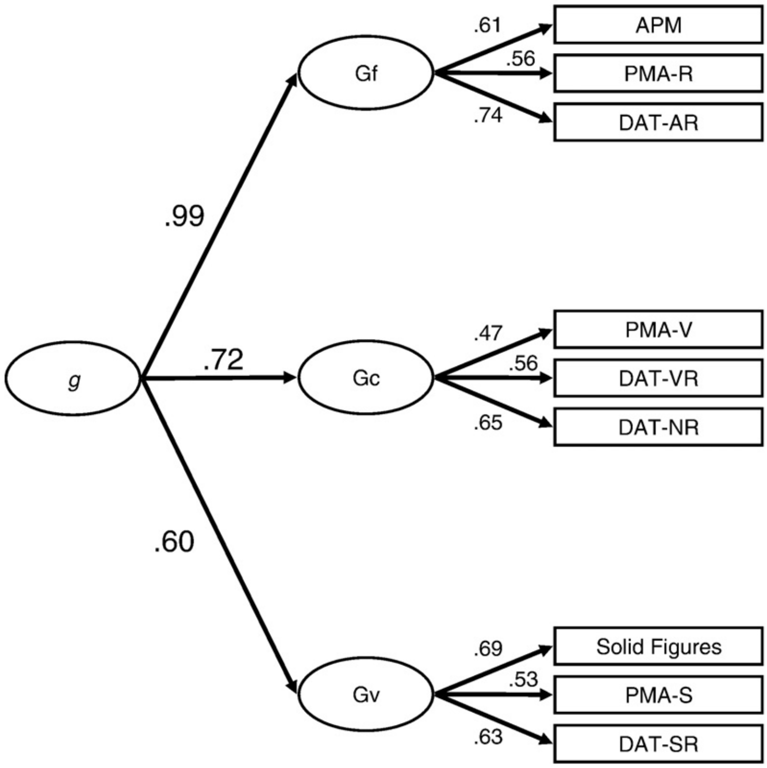

Fig. 2. CFA model for the considered psychometric measures of intelligence (APM = Advanced Progressive Matrices Test, PMA-R = inductive reasoning subtests from the PMA Battery, DAT-AR = abstract reasoning subtest from the DAT Battery, PMA-V = vocabulary subtests from the PMA Battery, DAT-VR = verbal reasoning subtest from the DAT Battery, DAT-NR = numerical reasoning subtest from the DAT Battery, PMA-S = mental rotation subtest from the PMA Battery, DAT-SR = spatial relations subtest from the DAT Battery). It can be seen that fluid intelligence (Gf) is perfectly predicted by the general intelligence higher-order factor (g).

Consortium for Brain Mapping, T1 452 Atlas, John C. Mazziotta and Arthur W. Toga, http://www.loni.ucla.edu/Atlases/Atlas_Detail.jsp?atlas_id=6). We removed the cerebellum prior to segmentation because its relatively high intensity can create inhomogeneity issues.

2. Results

2.1. Intelligence factors

Table 1 shows the descriptive statistics for the nine intelligence measures and the correlations among them. The correlation matrix was submitted to a confirmatory factor analysis (CFA) to test the postulated measurement model: three primary factors for Gf, Gc, and Gv were defined by their respective intelligence tests (see above). Further, a higher-order factor representing general intelligence (g) was also defined. The fit for this model was excellent: RMSEA=.000, $\chi^2_{(24)}$=23.4, χ^2/df=.97. Fig. 2 depicts the structural weights. Note that fluid intelligence (Gf) was the primary factor best predicted by the higher-order factor (g). Indeed, the measurement model shows that g=Gf.

In the next step, standardized scores (z) for the nine tests were used to compute averages for general intelligence (g), Gc, and Gv. A stepwise regression analysis was then computed using general intelligence as predictor, whereas Gc and Gv were the dependent scores. Gc and Gv variance unpredicted by the general intelligence score defined crystallized and spatial residual scores. This procedure resulted in three orthogonal scores for general intelligence (g), crystallized intelligence (Gc-r), and spatial intelligence (Gv-r). As Table 2 shows, general intelligence was related to all the measures, while Gc-r and Gv-r were related to their respective measures only.

2.2. Correlation of intelligence factors to gray matter (GM)

In the final analytic stage, the three orthogonal scores for general intelligence (g), Gc-r, and Gv-r were related to gray matter using SPM5 (sex was included as a nuisance variable). Tables A.1 to A.4 (see Appendix), as well as Figs. 3 to 5, show the results.

Table 2
Correlations among constructs and measures

	General intelligence	Gc-residual	Gv-residual
APM	.584**	−.084	−.061
PMA-R	.601**	.044	−.056
DAT-AR	.696**	.040	.117
PMA-V	.502**	.686**	.092
DAT-VR	.553**	.658**	.071
DAT-NR	.598**	.633**	.078
Solid figures	.588**	.107	.732**
PMA-S	.487**	.126	.747**
DAT-SR	.582**	.027	.662**

**p<.01.

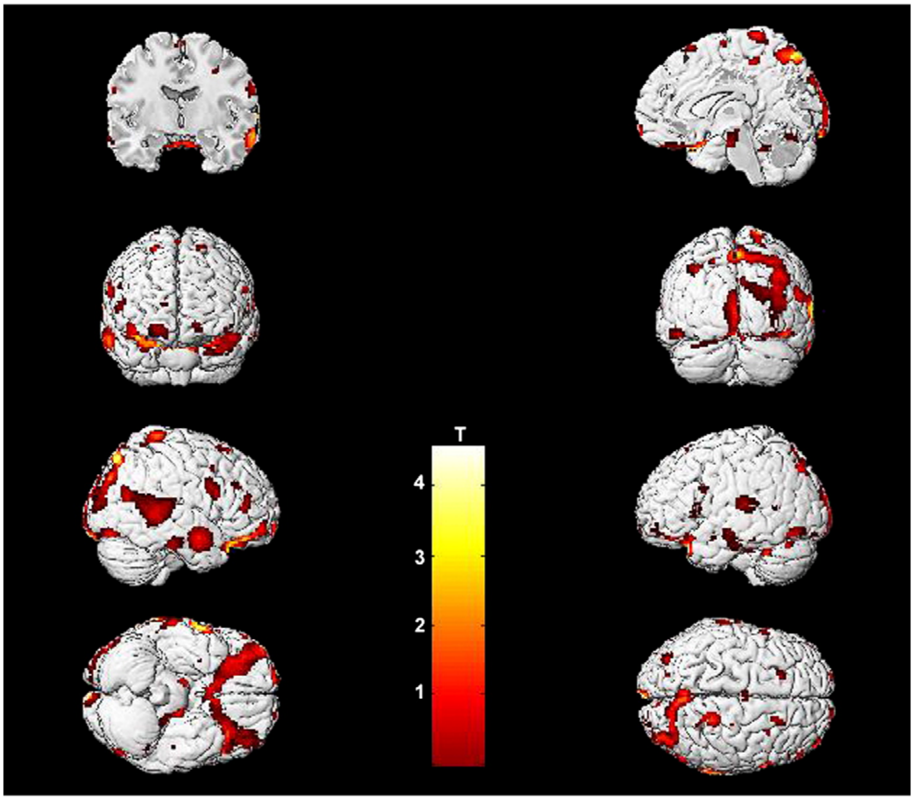

Fig. 3. Positive correlations between regional gray matter and general intelligence ($N=100$, $p<.005$, uncorrected for multiple comparisons). No negative correlations were found for this construct.

Table A.1 shows the localization of positive correlations between regional GM and general intelligence ($p<.005$, uncorrected for multiple comparisons). Several clusters distributed throughout the brain were positively correlated with individual differences in general intelligence (Fig. 3). These clusters were located in (a) frontal Brodmann areas (BAs) 5, 6, 8, 9, 10, 11, 45, 46, and 47; (b) parietal BAs 3 and 7; (c) temporal BAs 20, 21, 22, 36, 39, and 42; and (d) occipital BAs 18 and 19. The percent of total significant voxels related to general intelligence was: frontal (36%), parietal (4%), temporal (22%), occipital (34%), and limbic system (4%). No negative correlations were found.

Table A.2 presents the localization of correlations between regional GM and the pure estimate of crystallized intelligence (Gc-r) ($p<.005$, uncorrected for multiple comparisons). It should be noted that the obtained Gc-r scores are orthogonal to general intelligence and spatial intelligence (Gv-r).

As was found for general intelligence, several clusters distributed throughout the brain were positively related to Gc-r (Fig. 4). These clusters were located in (a) frontal BAs 8 and 11; (b) parietal BAs 5, 7, and 40; (c) temporal BAs 20, 21, 38, and 39; and (d) occipital BAs 18 and 19. The percent of total significant voxels related to Gc-r was: frontal (14%), parietal (10%), temporal (19%), occipital (40%), and limbic system (17%). No negative correlations were found.

Table A.3 shows the localization of positive correlations between regional GM and the pure estimate of spatial intelligence (Gv-r) ($p<.005$, uncorrected for multiple comparisons). Note that the obtained Gv-r scores are orthogonal to both general intelligence and Gc-r.

As was found for general intelligence and Gc-r, several clusters distributed throughout the brain were positively related to Gv-r (Fig. 5A). These clusters were located in (a) frontal BAs 6, 8, 9, 10, and 11; (b) parietal BAs 5, 7, and 40; (c) temporal BAs 22, 39, and 44; and (d) occipital BAs 17, 18, and 19. The percent of total significant voxels related to Gv-r is: frontal (61%), parietal (21%), temporal (16%), occipital (1%), and limbic system (1%).

There were some negative correlations between regional GM and spatial intelligence (see Table A.4 and Fig. 5B): (a) frontal BAs 6, 11, and 47; (b) parietal BA 2; (c) temporal BA 20; and (d) occipital BAs 17 and 18. The percent of total voxels was: frontal (16%), parietal (3%), temporal (2%), occipital (75%), and limbic system (4%).

2.3. Overlapping and non-overlapping areas

Fig. 6 shows a schematic overlap of clusters where GM correlated to general, crystallized, and spatial intelligence factors. These clusters were located in frontal BAs 8 and 11, parietal BAs 5 and 7, temporal BAs 20 and 39, and occipital BAs 18 and 19. There is also an overlapping cluster for Gv and Gc located in parietal BA 40.

Non-overlapping clusters for general intelligence are located in frontal BAs 45, 46, and 47, parietal BA 3, and temporal BAs 37 and 42. For crystallized intelligence the non-

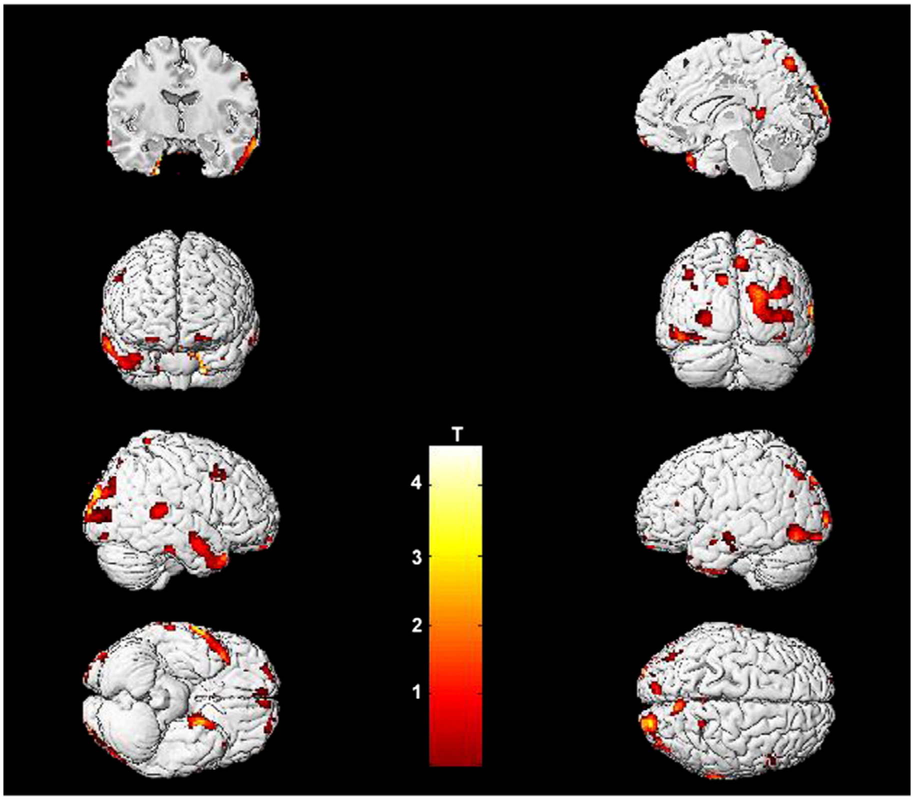

Fig. 4. Positive correlations between regional gray matter and the pure estimate of crystallized intelligence (N = 100, p < .005, uncorrected for multiple comparisons). No negative correlations were found for this construct.

overlapping cluster is located in temporal BA 38. Finally, for spatial intelligence, non-overlapping clusters are located in frontal BA 44 and occipital BA 17 (Fig. 6).

This descriptive schematic view suggests that (a) overlapping volumetric areas underlying general intelligence are distributed throughout the entire brain, (b) fluid and spatial

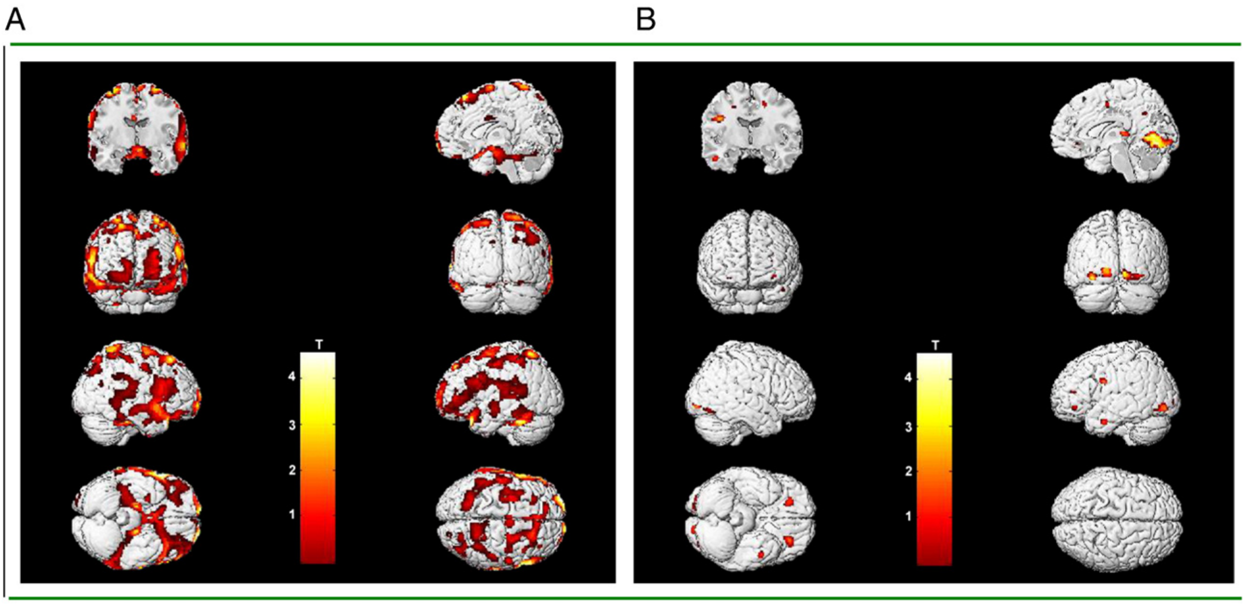

Fig. 5. A and B. Positive (A) and negative (B) correlations between regional gray matter and the pure estimate of spatial intelligence (N = 100, p < .005, uncorrected for multiple comparisons).

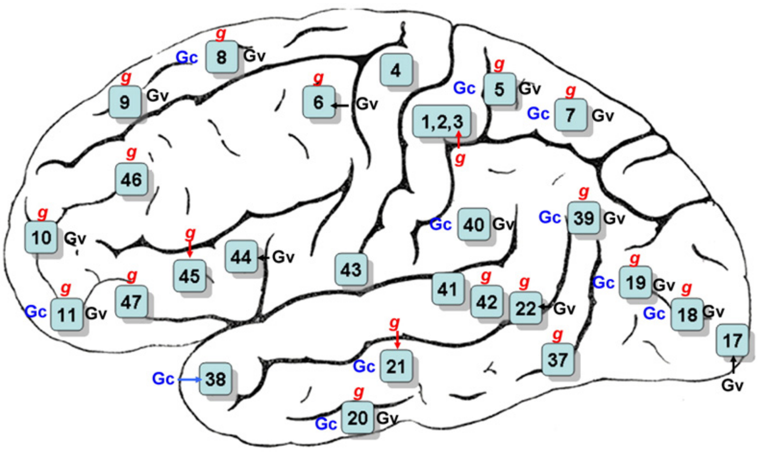

Fig. 6. Overlapping and non-overlapping clusters for general (*g*), crystallized (Gc-r), and spatial intelligence (Gv-r).Overlapping clusters concentrate on BAs 8 and 11 (frontal lobe), BA 5, 7, and 39 (parietal lobe), BA 20 (temporal lobe), and BAs 18 and 19 (occipital lobe). Non-overlapping clusters for Gf are focused on BAs 45–47 (frontal lobe), BA 3 (parietal lobe), and BAs 37 and 42 (temporal lobe). The non-overlapping cluster for Gc is observed in the temporal BA 38, whereas non-overlapping clusters for Gv are located in BA 44 (frontal lobe) and BA 17 (occipital lobe).

intelligence volumetric correlates are largely distributed, and (c) measures of crystallized intelligence correlate with volumes primarily within the temporal lobes.

3. Discussion

3.1. Relationship to P-FIT

The results reported here with respect to general intelligence are highly consistent with the parieto-frontal integration theory of intelligence (P-FIT) (Jung & Haier, 2007). Virtually all identified clusters of voxels correlating with the general intelligence score are located in brain areas underscored by the theoretical model (Figs. 1 and 6).

Nevertheless, there are small differences: clusters of voxels located in frontal Brodmann areas (BAs) 8 (frontal eye fields —involved in planning complex movements) and BA 11 (orbitofrontal area —implicated in reasoning, planning, and decision making), as well as in temporal BAs 20–21 (inferior and middle temporal gyrus, dedicated to high-level visual processing, recognition memory, auditory processing, and language), BA 36 (parahippocampal cortex, closely related to the fusiform gyrus), and BA 42 (auditory association cortex) were not included within the proposed theoretical model, but were identified in the present study.

Findings for the pure estimates of crystallized and spatial intelligence have not been reported before and warrant some comment. It is important to highlight that these estimates were uncorrelated with general (fluid) intelligence. Table 2 showed that general intelligence was related to all the measures in the battery, whereas the pure estimates for crystallized and spatial intelligence were related to their respective measures only. Therefore, findings for these latter estimates speak about verbal (Gc) and spatial (Gv) intelligence controlling for the pervasive influence of *g*.

We found overlapping clusters located in several brain areas for these two pure estimates of verbal and spatial intelligence, irrespective of the fact that their correlation is zero (Fig. 6): (a) frontal BAs 8 (frontal eye fields) and 11 (orbitofrontal area); (b) parietal BAs 5 and 7 (somato-sensory association cortex), and 40 (supramarginal gyrus part of Wernicke's area); (c) temporal BAs 20 (inferior temporal gyrus) and 39 (angular gyrus part of Wernicke's area), and (d) occipital BAs 18 and 19 (visual cortex). As noted above, most of these areas overlap with general intelligence, regardless of the fact that their correlation is also zero. This suggests that there might be common brain areas underlying individual differences in unrelated facets of the intelligence construct (see below).

3.2. The neuroanatomy of intelligence

The areas we find here related to intelligence have a number of theoretically relevant cognitive functions.

Frontal BAs 9–10 and 46 comprise the dorsolateral prefrontal cortex. This brain region is thought to play a role in sustaining attention and in working memory (Kane & Engle, 2002; Ramnani & Owen, 2004; Wager & Smith, 2003). Together with BA 11, it is involved in planning, reasoning, decision making, memory retrieval, and executive functioning. BA 45 includes Broca's area, and is implicated in semantic decision tasks, verb generation, and semantic working memory processes. It guides recovery of semantic information and evaluates this information within a given context. BA 47 is implicated in the processing of syntax. The role of BAs 5 (somato-sensory association cortex), 6 (pre-motor and supplementary motor cortex), and 8 (frontal eye fields) are less clear for intelligence. This latter area is involved in *planning* complex movements, so perhaps it can be considered that this region works in tandem with other frontal areas towards evaluation and hypothesis testing components. Further, assuming higher intelligence led to greater survival, these somato-sensory areas might have evolved together with “thinking” areas because they were important for running away effectively, articulating coping strategies, and so forth.

Parietal BA 7 (somato-sensory association cortex) is implicated in locating objects in space. Vision and proprioception converge on this brain area. BA 40 (supramarginal gyrus part of Wernicke's area) receives input from multiple sensory systems and may be a brain region involved in representation of integrated or abstract information (Cowan, 2005). BAs 3 (primary somato-sensory cortex) and 5 (somato-sensory association cortex) are also identified in the present study.

Temporal BAs 20 (inferior temporal gyrus), 21 (middle temporal gyrus), and 22 (superior temporal gyrus) are involved in high-level visual processing and recognition memory, auditory processing and language, and generation and understanding of individual words, respectively. BA 22 together with BAs 39–40 is where Wernicke's area lies. BA 36 (parahippocampal cortex) comprises the perirhinal cortex.

Finally, BAs 18 and 19 are visual association cortices. Together they comprise the extrastriate cortex, a brain area dedicated to feature-extraction, shape recognition, attentional and multimodal integrating functions.

Shaw's (2007) recent summary of the research regarding neuroimaging of intelligence is consistent with the generalist genes hypothesis, the P-FIT model, and the main results reported in the present article: *"the weight of evidence suggests intelligence is a distributed property of multiple interconnected cortical regions (…) the unitary theoretical construct of g may represent the emergent property of concerted action of a host of physiological and psychological processes"* (p. 964).

The dynamic model of general intelligence proposed by Van der Maas et al. (2007) based on a mathematically formulated developmental model relying on the so-called mutualism (i.e. positive beneficial relationships between cognitive processes) should also be considered within this framework. This model is thought to identify a plausible mechanism giving rise to the positive manifold behind *g*, but without including *g* as a latent factor. Van der Maas et al. (2007) suggest that psychometric *g* need not correspond to an actual quantitative variable, such as brain size. A similar model has been proposed by Dickens (2007) to account for the Flynn effect.

This is the important message: it is possible to empirically identify discrete brain areas wherein volumetric variations are related to the intelligence construct (Colom et al., 2006a,b, 2007; Frangou, Chitins, & Williams, 2004; Gong et al., 2005; Haier et al., 2004, 2005; Johnson et al., 2008; Wilke, Sohn, Byars, & Holland, 2003). Moreover, variations in the volume of these brain regions are clearly related to individual differences in intelligence in normal populations. Volumes of these brain structures are determined by the number and size of neurons. Therefore, greater volumes could implicate more efficient working structures.

The parieto-frontal integration theory (P-FIT) of intelligence is generally supported by the findings reported in the present article, and both are consistent with the generalist genes hypothesis. Results shown for the refined estimates of general (*g*), crystallized, and spatial intelligence are consistent with the view that cognitive abilities are supported by both common *and* unique discrete brain regions.

3.3. Looking ahead

There are some issues not explicitly addressed in the current study. Here we briefly discuss three of such issues. The first relates to the negative correlations observed for the pure estimate of spatial intelligence (Gv-r). These negative correlations mean that better scores on spatial intelligence covariate with smaller regional brain volumes on the identified clusters of voxels (see Table A.4 and Fig. 5B). While it is usually assumed that greater volumes should facilitate a more efficient cognition (Gong et al., 2005; Thompson et al., 2006), our negative correlations suggest that individual differences in spatial cognition do not always implicate greater volumes.

We may speculate briefly regarding this latter finding. More volume indicates more neurons, and more neurons provide more resources for cognition, perhaps leading to more efficient (i.e. less function) brain activity under some circumstances (Haier, Siegel, Tang, Abel, & Buscsbaum, 1992; Haier et al., 1988; Neubauer, Fink, & Schrausser, 2002). Developmental neural pruning may also be more effective for some cognitive development, although this needs more investigation (Shaw et al., 2006).

The second issue relates to the relevance of white matter for intelligence differences postulated by the P-FIT model. As noted above, white matter is thought to play a significant role for the reliable circulation of information across the entire brain. Actually, there are some studies reporting a significant contribution of regional variations in white matter to cognitive differences. Using VBM, Haier et al. (2004) found significant correlations between regional differences in white matter volumes at the temporal BA 39 and IQ. VBM, however, may not be the best technique for assessing white matter so we did not use it here. Two better techniques are Magnetic Resonance Spectroscopy (MRS) and Diffusion Tensor Imaging (DTI). Jung et al. (1999, 2005) used MRS and reported correlations between white matter integrity at BAs 39 and 40 (parietal lobe) and IQ scores in young adults. Schmithorst, Wilke, Dardzinski, and Holland (2005) found significant correlations between some cognitive functions and white matter architecture in a normal pediatric population using DTI. Also using DTI, Yu et al. (2008) found that patients with mental retardation show a general damage in the integrity of the brain white matter pathways they explored (corpus callosum, uncinate fasciculus, cingulum, optic radiation, and corticospinal tract). Further, participants with normal IQs (mean <120) showed less white matter integrity than Ss with high IQs (mean >120) on the uncinate fasciculus only. The uncinate fasciculus links the anterior part of the temporal lobe and the orbital gyrus (frontal lobe). Yu et al. (2008) speculate that this white matter tract is related to memory processes relevant for intelligent behaviour.

The P-FIT model underscores the arcuate fasciculus, a neural pathway connecting the posterior part of the temporo-parietal junction with the frontal cortex in the brain. Future studies with DTI and MRS will explore the probable association between intelligence and white matter variations on this pathway to explicitly test the prediction posited by this model.

Finally, several studies have reported substantial sex differences in brain structure as related to intelligence. Haier et al.'s (2005) study revealed that females show more white matter and fewer gray matter areas related to IQ. In males IQ/gray matter correlations were strongest in frontal and parietal lobes (BAs 8, 9, 39, 40), whereas the largest correlations in females were found in the frontal BA 10 (frontopolar area) and Broca's area. Interestingly, males and females achieve similar IQ results with different brain regions, suggesting that distinguishable brain designs may produce comparable intellectual achievements. Chen, Sachdev, Wen and Ansteyc (2007) examined sex-related differences in regional gray matter in 44–48 year old healthy individuals recruited from a random community sample ($N = 411$). Males had more gray matter volume in midbrain, left inferior temporal gyrus, right occipital lingual gyrus, right middle temporal gyrus, and both cerebellar hemispheres. Females had more gray matter in dorsal anterior, posterior and ventral cingulate cortices, and right inferior parietal lobule. These researchers endorse the view that these differences may provide the structural brain basis for sex differences in certain cognitive functions. Schmithorst and Holland (2007) investigated differences in boys and girls ($N = 300$) in the relationship between intelligence and functional connectivity for a task of narrative comprehension. Their results showed that for boys there was a greater association between intelligence and the functional connectivity linking Broca's area to auditory processing areas, including Wernicke's areas and the right posterior superior temporal gyrus. For girls, a greater association was observed between intelligence and the functional connectivity linking the left posterior superior temporal gyrus to Wernicke's areas in both hemispheres. Their results show a sexual dimorphism in the relationship of functional connectivity to intelligence. We will report sex differences using the present data set as well, but the scope of those analyses requires a separate report.

The application of neuroimaging to intelligence research is a relatively new field. Progress is accelerating as studies with large sample sizes incorporate more refined approaches for the measurement of intelligence, new technical developments, like Diffusion Tensor Imaging and Magnetic Resonance Spectroscopy, and key differential factors like sex and age. The data reported here provide support for the P-FIT model and demonstrate there is still much work to do before detailing the neuro-anatomic bases of intelligence and its basic factors.

Acknowledgement

This work was funded by the grant SEJ-2006-07890 from the *Ministerio de Educación y Cultura* (MEC) [Ministry of Education and Culture].

Appendix A. Localization of correlations between regional gray matter and the measures of interest

Table A.1
Localization of positive correlations ($p < .005$) between regional gray matter and general intelligence (see Fig. 3)

Brain regions$	*x*, *y*, *z* coordinates	Cluster size
Left frontal		
BA 6 (superior frontal gyrus)	20, 28, 59	31
BA 10 (superior frontal gyrus)	− 16, 69, − 12	68
BA 6 (medial frontal gyrus)	0, − 5, 63	32
BA 45 (inferior frontal gyrus)	− 61, 18, 3	40
BA 45 (inferior frontal gyrus)	− 57, 11, 23	19
BA 6 (medial frontal gyrus)	− 6, − 21, 51	4
Right frontal		
BA 11 (rectal gyrus)	6, 10, − 24	2400*
BA 47 (inferior frontal gyrus)	− 34, 28, − 23	
BA 11 (middle frontal gyrus)	32, 36, − 22	
BA 9 (inferior frontal gyrus)	65, 13, 27	128
BA 8 (middle frontal gyrus)	32, 14, 40	20
BA 11 (superior frontal gyrus)	22, 67, − 17	168
BA 46 (middle frontal gyrus)	55, 36, 26	127
BA 46 (inferior frontal gyrus)	57, 41, 9	
BA 46 (middle frontal gyrus)	53, 45, 16	
BA 5 (paracentral lobule)	10, − 32, 50	56
BA 6 (superior frontal gyrus)	26, 28, 58	54
BA 10 (superior frontal gyrus)	14, 70, 9	11
BA 6 (precentral gyrus)	26, − 15, 54	7
Total voxels frontal lobe		3165
Left parietal		
BA 7 (superior parietal lobule)	− 36, − 75, 46	147*
BA 19 (superior occipital gyrus)	− 36, − 86, 36	
BA 7 (precuneus)	− 18, − 73, 52	19
Right parietal		
BA 3 (postcentral gyrus)	20, − 33, 72	184*
BA 7 (superior parietal lobule)	26, − 47, 63	
Total voxels parietal lobe		350
Left temporal		
BA 42 (superior temporal gyrus)	− 71, − 26, 14	323*
BA 21 (middle temporal gyrus)	− 69, − 54, 12	
BA 20 (inferior temporal gyrus)	− 69, − 20, − 21	225
BA 21 (middle temporal gyrus)	− 71, − 12, − 13	
BA 21 (middle temporal gyrus)	− 65, 1, − 14	
BA 36 (fusiform gyrus)	− 42, − 48, − 25	54
BA 20 (fusiform gyrus)	− 44, − 22, − 16	7
Right temporal		
BA 22 (superior temporal gyrus)	71, − 37, 6	837*
BA 39 (superior temporal gyrus)	57, − 63, 23	
BA 39 (superior temporal gyrus)	65, − 61, 21	
BA 21 (middle temporal gyrus)	67, 1, − 19	488*
BA 20 (inferior temporal gyrus)	69, − 25, − 24	
BA 20 (inferior temporal gyrus)	63, − 34, − 25	
BA 20 (fusiform gyrus)	26, − 46, − 20	47
BA 20 (inferior temporal gyrus)	34, − 2, − 44	6
Total voxels temporal lobe		1987
Left occipital		
BA 18 (inferior occipital gyrus)	− 42, − 92, − 7	453*
BA 19 (middle occipital gyrus)	− 55, − 72, − 8	
BA 18 (middle occipital gyrus)	− 36, − 99, 9	
Lingual gyrus	− 12, − 67, − 13	79
Fusiform gyrus	− 24, − 67, − 17	
BA 19 (fusiform gyrus)	− 32, − 65, − 19	
Right occipital		
BA 18 (lingual gyrus)	4, − 99, − 5	2444*
BA 18 (cuneus)	0, − 102, 11	
BA 7 (precuneus)	0, − 57, 54	
Lingual gyrus	6, − 65, − 10	26
Total voxels occipital lobe		3002
Left limbic lobe		
BA 30 (parahippocampal gyrus)	− 6, − 39, − 3	147
BA 28 (parahippocampal gyrus)	− 14, − 20, − 21	103
BA 36 (parahippocampal gyrus)	− 22, − 32, − 22	
BA 23 (cingulate gyrus)	− 6, − 14, 28	15
Right limbic lobe		
BA 34 (parahippocampal gyrus)	12, − 14, − 16	67
Substantia nigra	16, − 20, − 7	
Total voxels limbic lobe		332

$Brain regions (approximate Brodmann areas, BAs) are estimated from Talairach and Tournoux (1988) atlas. Coordinates refer to maximum voxel of identified clusters. Cluster size is number of voxels with a significant correlation to the intelligence score (a blank size indicates a subcluster of the preceding major cluster). *$p < .0001$.

Table A.2
Localization of positive correlations ($p<.005$) between regional gray matter and crystallized intelligence (see Fig. 4)

Brain regions$	x, y, z coordinates	Cluster size
Left frontal		
Inferior frontal gyrus	− 28, 32, 11	38
BA 11 (superior frontal gyrus)	− 22, 63, − 18	122
Right frontal		
BA 11 (superior frontal gyrus)	4, 55, − 28	215*
BA 11 (superior frontal gyrus)	26, 63, − 18	105*
BA 8 (middle frontal gyrus)	55, 19, 40	121
BA 11 (rectal gyrus)	4, 10, − 24	27
BA 11 (superior frontal gyrus)	28, 42, − 21	2
Total voxels frontal lobe		630
Left parietal		
BA 19 (precuneus)	− 42, − 75, 46	180
BA 40 (inferior parietal lobule)	− 48, − 63, 51	
BA 19 (superior occipital gyrus)	− 36, − 86, 36	
BA 19 (precuneus)	− 10, − 85, 41	96
Right parietal		
BA 7 (precuneus)	4, − 61, 53	133
BA 5 (postcentral gyrus)	24, − 41, 72	29
Total voxels parietal lobe		438
Left temporal		
BA 21 (middle temporal gyrus)	− 71, − 12, − 11	143
BA 21 (middle temporal gyrus)	− 63, 1, − 15	
BA 21 (middle temporal gyrus)	− 69, − 18, − 19	
BA 39 (middle temporal gyrus)	− 55, − 67, 27	22
BA 38 (superior temporal gyrus)	− 40, 22, − 28	6
Right temporal		
BA 22 (superior temporal gyrus)	69, − 34, 13	185*
BA 21 (middle temporal gyrus)	65, − 1, − 17	472
BA 38 (superior temporal gyrus)	40, 24, − 28	
BA 38 (superior temporal gyrus)	46, 18, − 35	
BA 20 (inferior temporal gyrus)	71, − 28, − 20	60
Total voxels temporal lobe		888
Left occipital		
BA 19 (middle occipital gyrus)	− 53, − 72, − 3	477*
BA 18 (inferior occipital gyrus)	− 44, − 82, − 6	
BA 18 (middle occipital gyrus)	− 26, − 99, 9	189*
BA 18 (middle occipital gyrus)	− 24, − 88, 21	4
Right occipital		
BA 19 (cuneus)	22, − 90, 28	1118*
BA 19 (middle occipital gyrus)	22, − 96, 18	
BA 18 (middle occipital gyrus)	30, − 99, 10	
BA 18 (inferior occipital gyrus)	42, − 84, − 6	23
Total voxels occipital lobe		1811
Left limbic lobe		
Posterior cingulate	− 2, − 38, 9	223*
BA 38 (uncus)	− 20, 8, − 39	532
BA 28 (uncus)	− 14, 3, − 27	
BA 36 (uncus)	− 18, − 8, − 38	
Right limbic lobe		
BA 36 (uncus)	18, − 5, − 32	39
Total voxels limbic lobe		794

$Brain regions (approximate Brodmann areas, BAs) are estimated from Talairach and Tournoux (1988) atlas. Coordinates refer to maximum voxel of identified clusters. Cluster size is number of voxels with a significant correlation to the intelligence score (a blank size indicates a subcluster of the preceding major cluster).
*$p<.0001$.

Table A.3
Localization of positive correlations ($p<.005$) between regional gray matter and spatial intelligence (see Fig. 5A)

Brain regions$	x, y, z coordinates	Cluster size
Left frontal		
BA 10 (superior frontal gyrus)	− 26, 68, − 3	8765*
BA 11 (rectal gyrus)	− 8, 12, − 24	
BA 22 (superior temporal gyrus)	− 69, − 44, 17	
BA 8 (superior frontal gyrus)	− 28, 34, 52	106
Right frontal		
BA 6 (middle frontal gyrus)	28, 5, 64	1457*
BA 6 (superior frontal gyrus)	22, 28, 54	
BA 8 (superior frontal gyrus)	30, 32, 50	
BA 6 (superior frontal gyrus)	4, − 1, 66	215*
BA 10 (superior frontal gyrus)	10, 70, 4	731*
BA 10 (superior frontal Gyrus)	26, 65, − 12	
BA 10 (Superior Frontal gyrus)	16, 69, − 10	
BA 9 (middle frontal gyrus)	38, 39, 35	25
Total voxels frontal lobe		11,299
Left parietal		
BA 7 (superior parietal lobule)	− 22, − 59, 66	1601*
BA 6 (middle frontal gyrus)	− 30, 3, 64	
BA 40 (inferior parietal lobule)	− 49, − 36, 59	
BA 19 (precuneus)	− 10, − 87, 41	14
Right parietal		
BA 5 (postcentral gyrus)	22, − 43, 70	714*
BA 7 (postcentral gyrus)	12, − 47, 72	
BA 5 (postcentral gyrus)	40, − 45, 63	
BA 19 (precuneus)	46, − 72, 44	1535
BA 40 (postcentral gyrus)	69, − 21, 16	
BA 7 (superior parietal lobule)	26, − 69, 59	
Total voxels parietal lobe		3864
Left temporal		
BA 39 (middle temporal gyrus)	− 49, − 80, 30	36
Right temporal		
BA 22 (superior temporal gyrus)	57, 11, − 7	2932*
BA 44 (inferior frontal gyrus)	61, 18, 16	
BA 11 (superior frontal gyrus)	24, 40, − 24	
Total voxels temporal lobe		2968
Left occipital		
BA 18 (inferior occipital gyrus)	− 42, − 93, − 4	48
Right occipital		
BA 17 (inferior occipital gyrus)	28, − 96, − 10	70
BA 18 (inferior occipital gyrus)	36, − 94, − 9	
Total voxels occipital lobe		118
Left limbic lobe		
BA 24 (cingulate gyrus)	− 4, − 1, 28	90
Right limbic lobe		
BA 20 (uncus)	26, − 4, − 40	110
Total voxels limbic lobe		200

$Brain regions (approximate Brodmann areas, BAs) are estimated from Talairach and Tournoux (1988) atlas. Coordinates refer to maximum voxel of identified clusters. Cluster size is number of voxels with a significant correlation to the intelligence score (a blank size indicates a subcluster of the preceding major cluster).
*$p<.0001$.

Table A.4
Localization of negative correlations (p<.005) between regional gray matter and spatial intelligence (see Fig. 5B)

Brain regions$	x, y, z coordinates	Cluster size
Left frontal		
BA 6 (precentral gyrus)	− 40 − 1 26	119*
BA 47 (inferior frontal gyrus)	− 26 33 − 5	131
Medial frontal gyrus	− 26 37 9	31
BA 6 (middle frontal gyrus)	− 22 − 2 41	9
Right frontal		
BA 11 (middle frontal gyrus)	26 37 − 7	98
Total voxels frontal lobe		388
Left parietal		
Right parietal		
BA 2 (postcentral gyrus)	34 − 23 36	67
Precuneus	22 − 53 34	23
Total voxels parietal lobe		90
Left temporal		
BA 20 (fusiform gyrus)	− 46 − 3 − 22	49
Right temporal		
Total voxels temporal lobe		49
Left occipital		
BA 17 (cuneus)	− 16 − 77 6	728
BA 18 (inferior occipital gyrus)	− 34 − 82 − 3	
BA 17 (lingual gyrus)	− 12 − 89 4	
Right occipital		
BA 18 (right lingual gyrus)	20 − 70 5	1131*
Right middle occipital gyrus	30 − 87 − 1	
Total voxels occipital lobe		1859
Left limbic lobe		
Right limbic lobe		
Pulvinar (thalamus)	16 − 29 9	74
BA 24 (cingulate gyrus)	20 − 4 44	27
Total voxels limbic lobe		101

$Brain regions (approximate Brodmann areas, BAs) are estimated from Talairach and Tournoux (1988) atlas. Coordinates refer to maximum voxel of identified clusters. Cluster size is number of voxels with a significant correlation to the intelligence score (a blank size indicates a subcluster of the preceding major cluster).
*p<.0001.

References

Ashburner, J., & Friston, K. J. (2000). Voxel-based morphometry —The methods. *Neuroimage*, *11*, 805−821.

Colom, R. (2007). Intelligence? What intelligence? *Behavioural and Brain Sciences*, *30*, 155−156.

Colom, R., Abad, F. J., Quiroga, MaA., Shih, P. C., & Flores-Mendoza, C. (in press). Working memory and intelligence are highly related constructs, but why? *Intelligence*.

Colom, R., Jung, R. E., & Haier, R. J. (2006). Finding the *g*-factor in brain structure using the method of correlated vectors. *Intelligence*, *34*, 561−570.

Colom, R., Jung, R. E., & Haier, R. J. (2006). Distributed brain sites for the g-factor of intelligence. *Neuroimage*, *31*, 1359−1365.

Colom, R., Jung, R. E., & Haier, R. J. (2007). General intelligence and memory span: Evidence for a common neuro-anatomic framework. *Cognitive Neuropsychology*, *24*(8), 867−878.

Cowan, N. (2005). *Working memory capacity.* New York: Psychology Press.

Chen, X., Sachdev, P. S., Wen, W., & Ansteyc, K. J. (2007). Sex differences in regional gray matter in healthy individuals aged 44–48 years: A voxel-based morphometric study. *NeuroImage*, *36*, 691−699.

Dickens, W.T. (2007). What is *g*? Paper presented at the 2nd Scheeling Symposium. University of Maryland, November 19 2007.

Draganski, B., Gaser, C., Busch, V., Schuierer, G., Bogdahn, U., & May, A. (Jan. 2004). Changes in grey matter induced by training. *Nature*, *427*, 311−312.

Frangou, S., Chitins, X., & Williams, S. C. R. (2004). Mapping IQ and gray matter density in healthy young people. *Neuroimage*, *23*, 800−805.

Garlick, D. (2003). Integrating brain science research with intelligence research. *Current Directions in Psychological Science*, 185−189.

Gong, Q. -Y., Sluming, V., Mayes, A., Keller, S., Barrick, T., Cezayirli, E., et al. (2005). Voxel-based morphometry and stereology provide convergent evidence of the importance of medical prefrontal artex for fluid intelligence in healthy adults. *Neuroimage*, *25*, 1175−1186.

Good, C. D., Johnsrude, I. S., Ashburner, J., Henson, R. N., Friston, K. J., & Frackowiak, R. S. (2001). A voxel-based morphometric study of ageing in 465 normal adult human brains. *Neuroimage*, *14*, 21−36.

Haier, R. J., & Jung, R. E. (2007). Beautiful minds (i.e. brains) and the neural basis of intelligence. *Behavioral and Brain Sciences*, *30*, 174−178.

Haier, R. J., Jung, R. E., Yeo, R. A., Head, K., & Alkire, M. T. (2004). Structural brain variation and general intelligence. *NeuroImage*, *23*, 425−433.

Haier, R. J., Jung, R. E., Yeo, R. A., Head, K., & Alkire, M. T. (2005). The neuroanatomy of general intelligence: Sex matters. *Neuroimage*, *25*, 320−327.

Haier, R. J., Siegel, B. V., Nuechterlein, K. H., Hazlett, E., Wu, J. C., Paek, J., et al. (1988). Cortical glucose metabolic rate correlates of abstract reasoning and attention studied with Positron Emission Tomography. *Intelligence*, *12*, 199−217.

Haier, R. J., Siegel, B., Tang, C., Abel, L., & Buscsbaum, M. S. (1992). Intelligence and changes in regional cerebral glucose metabolic rate following learning. *Intelligence*, *16*, 415−426.

Johnson, W., Jung, R. E., Colom, R., & Haier, R. J. (2008). Cognitive abilities independent of IQ correlate with regional brain structure. *Intelligence*, *36*, 18−28.

Jung, R. E., & Haier, R. J. (2007). The Parieto-Frontal Integration Theory (P-FIT) of intelligence: Converging neuroimaging evidence. *Behavioral and Brain Sciences*, *30*, 135−187.

Jung, R. E., Haier, R. J., Yeo, R. A., Rowland, L. M., Petropoulos, H., Levine, A. S., et al. (2005). Sex differences in *N*-acetylaspartate correlates of general intelligence: An ^{1}H-MRS study of normal human brain. *NeuroImage*, *26*, 965−972.

Jung, R. E., Yeo, R. A., Chiulli, S. J., Sibbitt, W. L., Jr., Weers, D. C., Hart, B. L., et al. (1999). Biochemical markers of cognition: A proton MR spectroscopy study of normal human brain. *NeuroReport*, *10*, 3327−3331.

Kane, M. J., & Engle, R. W. (2002). The role of prefrontal cortex in working-memory capacity, executive attention, and general fluid intelligence: An individual-differences perspective. *Psychonomic Bulletin & Review*, *9*, 637−671.

Kovas, Y., & Plomin, R. (2006). Generalist genes: Implications for the cognitive sciences. *Trends in Cognitive Sciences*, *10*, 198−203.

Neubauer, A. C., Fink, A., & Schrausser, D. G. (2002). Intelligence and neural efficiency: The influence of task content and sex on the brain–IQ relationship. *Intelligence*, *30*, 515−536.

Posthuma, D., Baare, W. F., Pol, H. E. H., Kahn, R. S., Boomsma, D. I., & De Geus, E. J. (2003). Genetic correlations between brain volumes and the WAIS-III dimensions of verbal comprehension, working memory, perceptual organization, and processing speed. *Twin Research*, *6*, 31−39.

Ramnani, N., & Owen, A. M. (2004). Anterior prefrontal cortex: Insights into function from anatomy and neuroimaging. *Nature Neuroscience*, *5*, 184−194.

Schmithorst, V. J., & Holland, S. K. (2007). Sex differences in the development of neuroanatomical functional connectivity underlying intelligence found using Bayesian connectivity analysis. *Neuroimage*, *35*, 406−419.

Schmithorst, V. J., Wilke, M., Dardzinski, B. J., & Holland, S. K. (2005). Cognitive functions correlate with white matter architecture in a normal pediatric population: A Diffusion Tensor MRI Study. *Human Brain Mapping*, *26*, 139−147.

Shaw, P. (2007). Intelligence and the developing human brain. *BioEssays*, *29*, 962−973.

Shaw, P., Greenstein, D., Lerch, J., Clasen, L., Lenroot, R., Gogtay, N., et al. (2006). Intellectual ability and cortical development in children and adolescents. *Nature*, *440*, 676−679.

Talairach, J., & Tournoux, P. (1988). *Co-planar stereotaxic atlas of the human brain: A 3-dimmensional proportional system, an approach to cerebral imaging.* New York: Thieme Medical Publishers.

Thompson, P. M., Cannon, T. D., Narr, K. L., van Erp, T., Poutanen, V. P., Huttunen, M., et al. (2001). Genetic influences on brain structure. *Nature Neuroscience*, *4*(12), 1253−1258.

Thompson, P. M., Hayashi, K. M., Dutton, R. A., Chiang, M. C., Leow, A. D., Sowell, E. R., & Zubicaray, G. (2006). Tracking Alzheimer's Disease. *Annals of the New York Academy of Sciences*, 185−189.

Toga, A. W., & Thompson, P. M. (2005). Genetics of brain structure and intelligence. *Annual Review of Neuroscience*, *28*, 1−23.

Toga, A. W., & Thompson, P. M. (2007). What is where and why it is important. *NeuroImage*, *37*, 1045−1049.

Van der Maas, H., Dolan, C. V., Grasman, R. P. P. P., Wicherts, J. M., Huizenga, H. M., & Raijmakers, M. E. J. (2007). A dynamical model of general intelligence: The positive manifold of intelligence by mutualism. *Psychological Review*, *113*, 842−861.

Wager, T. D., & Smith, E. E. (2003). Neuroimaging studies of working memory: A meta-analysis. *Cognitive, Affective, and Behavioral Neuroscience*, *3*, 255−274.

Wilke, M., Sohn, J. H., Byars, A. W., & Holland, S. K. (2003). Bright spots: correlations of gray matter volume with IQ in a normal pediatric population. *Neuroimage*, *20*, 202−215.

Yu, Ch., Li, J., Liu, Y., Qin, W., Li, Y., Shu, N., et al. (2008). White matter tract integrity and intelligence in patients with mental retardation and healthy adults. *NeuroImage*, *40*, 1533−1541.